

## Supplementary Materials for

### Direct measurements of DOCO isomers in the kinetics of OD + CO

Thinh Q. Bui, Bryce J. Bjork, P. Bryan Changala, Thanh L. Nguyen, John F. Stanton, Mitchio Okumura, Jun Ye

Published 12 January 2018, *Sci. Adv.* **4**, eaao4777 (2018)

DOI: 10.1126/sciadv.aao4777

#### This PDF file includes:

- section S1. *cis*-DOCO isotope shift and spectral parameters
- section S2.  $k_{1a, \text{sum}}$  fitting
- section S3. Theoretical calculations for OD + CO
- section S4.  $k_1$  for OD + CO as a function of  $\text{N}_2$
- table S1. Experimental spectral features for *cis*- $\text{DO}^{12}\text{CO}$  and *cis*- $\text{DO}^{13}\text{CO}$  and their rovibrational assignments.
- table S2. Summary of spectral parameters for *cis*- $\text{DO}^{12}\text{CO}$  and *cis*- $\text{DO}^{13}\text{CO}$ .
- table S3. Comparison of experimental and theoretical isotopic shifts for *cis*-DOCO.
- table S4. Summary of statistical and systematic errors for  $k_{1a, \text{sum}}$ .
- table S5. Summary of fitted rate coefficients.
- fig. S1. Variation of  $r_{\text{loss, sum}}$  with  $\text{O}_3$  concentration.
- fig. S2. Variation of  $k_{1a, \text{sum}}$  with  $\text{D}_2$  concentration.
- fig. S3. Calculated *cis/trans* isomerization rates for DOCO isomers using SCTST and 2D master equations.
- fig. S4. Measured  $k_1$  comparison with previous works.

## Supplementary Materials

### section S1. *cis*-DOCO isotope shift and spectral parameters

The experimental *cis*-DO<sup>12</sup>CO and *cis*-DO<sup>13</sup>CO spectra are presented in Fig. 2A. Compiled in table S1 are the observed transitions and their approximate transition frequencies in wavenumber (cm<sup>-1</sup>). Due to Doppler (~300 MHz) and instrumental (~900 MHz) broadening, we are not able to resolve the individual rotational features of each Q-branch.

**table S1. Experimental spectral features for *cis*-DO<sup>12</sup>CO and *cis*-DO<sup>13</sup>CO and their rovibrational assignments.** The quantity in parenthesis provides an estimate of the uncertainty in the line position (in cm<sup>-1</sup>) due to the FWHM linewidth of the unresolved Q-branch feature.

K <sub>a</sub> '	K <sub>a</sub> ''	<sup>12</sup> C Position (cm <sup>-1</sup> )	<sup>13</sup> C Position (cm <sup>-1</sup> )
7	8	2489.220(0.147)*	2491.106(0.147)*
6	7	2496.040(0.08)	2497.718(0.08)
5	6	2502.931(0.05)	2504.295(0.05)
4	5	2509.764(0.05)	--
3	4	2516.524(0.05)	2517.282(0.05)
2	3	--	--
1	2	--	--
2	1	2548.102(N/A)*	2547.572(N/A)*
3	2	--	--
4	3	2562.550(0.13)	2561.517(0.13)
5	4	2568.954(0.11)	2567.638(0.11)
6	5	2575.191(0.10)	2573.687(0.10)
7	6	2581.414(0.10)	2579.658(0.10)
8	7	--	--

\*not fitted

--transitions are too blended and/or SNR<2:1

By fitting the observed transitions to a Watson A-reduced asymmetric top Hamiltonian using PGOPHER, we obtain the vibrational band origin and A rotational constant (table S2).

**table S2. Summary of spectral parameters for *cis*-DO<sup>12</sup>CO and *cis*-DO<sup>13</sup>CO.** The average fit error is 0.014 cm<sup>-1</sup>.

	<sup>12</sup> C(v=0)	<sup>12</sup> C(v=1)	<sup>13</sup> C(v=0)	<sup>13</sup> C(v=1)
Origin (cm <sup>-1</sup> )	0	2539.909(3)	0	2539.725(4)
A (MHz)	110105.52 <sup>a</sup>	109313(4)	106124(5)	105423(5)
B (MHz)	11423.441 <sup>a</sup>	11422.882 <sup>b</sup>	11420.075 <sup>c</sup>	11419.559 <sup>d</sup>
C (MHz)	10331.423 <sup>a</sup>	10324.228 <sup>b</sup>	10291.999 <sup>c</sup>	10284.951 <sup>d</sup>

<sup>a</sup>McCarthy *et al.* 2016

<sup>b</sup><sup>12</sup>C(v=0) value + VPT2 vibrational shifts

<sup>c</sup><sup>12</sup>C(v=0) value + VPT2 isotopic shift

<sup>d</sup><sup>12</sup>C(v=0) value + VPT2 isotopic shift & vibrational shift

**table S3. Comparison of experimental and theoretical isotopic shifts for *cis*-DOCO.**

	Experiment	Theory
Vibrational Shift (MHz)		
<sup>12</sup> C	-793(4)	-877.296
<sup>13</sup> C	-701(7)	-797.649
Isotopic Shift (MHz)		
v=0	-3982(5)	-3976.926
v=1	-3890(6)	-3897.279
isotopic shift in band origin (cm <sup>-1</sup> )	-0.184	-0.207 <sup>e</sup>
		-0.16 <sup>f</sup>

<sup>e</sup>VPT2

<sup>f</sup>variational calculation

## section S2. *k*<sub>1a,sum</sub> fitting

At early times ( $t < 200 \mu\text{s}$ ), the *cis*- and *trans*-DOCO time dependence are described by the first-order differential equations

$$\begin{aligned} \frac{d[cis]}{dt} &= k_{1a,cis} [CO][OD]_t - (k_{\text{loss},cis} [X] + k_{\text{iso},ct}) [cis]_t + k_{\text{iso},tc} [trans]_t \\ \frac{d[trans]}{dt} &= k_{1a,trans} [CO][OD]_t - (k_{\text{loss},trans} [X] + k_{\text{iso},tc}) [trans]_t + k_{\text{iso},ct} [cis]_t \end{aligned} \quad (\text{S1})$$

where  $k_{iso,ct}$  and  $k_{iso,tc}$  are the *cis*→*trans* and *trans*→*cis* isomerization rate coefficients, respectively. The subscript  $t$  denotes time dependence.  $[OD]_t$ ,  $[cis]_t$ , and  $[trans]_t$  are the time-dependent concentrations of OD, *cis*-DOCO, and *trans*-DOCO, respectively, in the ground vibrational state.  $k_{loss,cis}$  and  $k_{loss,trans}$  are bimolecular loss rate coefficients for *cis*- and *trans*-DOCO, respectively, with one or more species X. By making the approximation that  $k_{loss,cis} = k_{loss,trans} = k_{loss,sum}$ , the rate equation for the sum of DOCO isomers is given by

$$\frac{d[\text{DOCO}_{\text{sum}}]}{dt} = k_{1a,\text{sum}} [\text{CO}][\text{OD}]_t - k_{\text{loss},\text{sum}} [\text{DOCO}_{\text{sum}}]_t [\text{X}] \quad (\text{S2})$$

Here,  $[\text{DOCO}_{\text{sum}}] \equiv [\text{trans}] + [\text{cis}]$  and  $k_{1a,\text{sum}} \equiv k_{1a,\text{cis}} + k_{1a,\text{trans}}$ . The isomerization terms from Eq. S1 cancel out when only the total concentration of DOCO is considered. The Laplace transform of Eq. S2 gives the solution in Eq. S3, which is the convolution of DOCO loss term with  $[\text{OD}]_t$

$$[\text{DOCO}_{\text{sum}}]_t = k_{1a,\text{sum}} [\text{CO}] \int_0^t e^{-(k_{\text{loss},\text{sum}}[\text{X}](t-u))} [\text{OD}](u) du \quad (\text{S3})$$

Here,  $u$  is a dummy variable. To fit the data, we use the empirical functional form of  $[\text{OD}]_t$  comprised of sum of exponential rise and fall components

$$[\text{OD}]_t = a_1 e^{-b_1 t} + a_2 e^{-b_2 t} - (a_1 + a_2) e^{-b_3 t} \quad (\text{S4})$$

Here,  $b_1$  and  $b_2$  are bi-exponential decay terms while  $b_3$  is a rise term. This procedure is equivalent to a spline interpolation in which  $a_1$ ,  $a_2$ ,  $b_1$ ,  $b_2$ , and  $b_3$  are fitted independently. Using Eq. S4, Eq. S3 is given by

$$[\text{DOCO}_{\text{sum}}]_t = k_{1a,\text{sum}}[\text{CO}] \left( a_1 \frac{e^{-b_1 t} - e^{-r_{\text{loss,sum}} t}}{b_1 - r_{\text{loss,sum}}} + a_2 \frac{e^{-b_2 t} - e^{-r_{\text{loss,sum}} t}}{b_2 - r_{\text{loss,sum}}} - (a_1 + a_2) \frac{e^{-b_3 t} - e^{-r_{\text{loss,sum}} t}}{b_3 - r_{\text{loss,sum}}} \right) \quad (\text{S5})$$

We fit Eqs. S4 and S5 to the measured  $[\text{OD}]_t$  and  $[\text{DOCO}]_t$  to obtain the  $\text{DOCO}_{\text{sum}}$  formation and loss rate coefficients,  $k_{1a,\text{sum}}$  and  $r_{\text{loss,sum}}$ , respectively. From our fitted values of the bimolecular rate coefficients  $k_{1a,\text{sum}}$ , we determined the termolecular rate coefficients from a multidimensional linear regression to the expression

$$k_{1a,\text{sum}} = k_{1a,\text{sum}}^{(\text{CO})} [\text{CO}] + k_{1a,\text{sum}}^{(\text{N}_2)} [\text{N}_2] + k_{1a,\text{sum}}^{(\text{D}_2)} [\text{D}_2] + k_{1a,\text{sum}}^{(0)} \quad (\text{S6})$$

The rate equation for the OD time dependence is

$$\frac{d[\text{OD}]}{dt} = k_{\text{D}_2} [\text{D}_2] [\text{O}(\text{D})]_t + k_{\text{O}_3} [\text{O}_3] [\text{D}]_t - (k_{1a,\text{cis}} + k_{1a,\text{trans}} + k_{1b}) [\text{CO}] [\text{OD}]_t \quad (\text{S7})$$

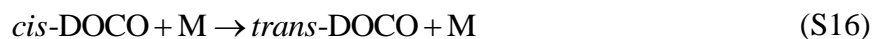
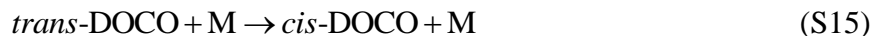
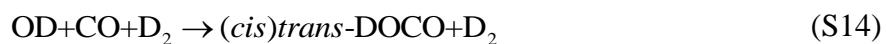
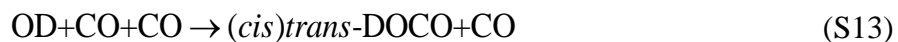
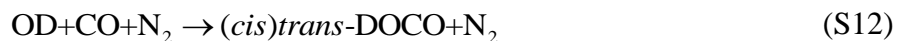
Here, the  $k_{\text{D}_2}$  ( $1.2 \times 10^{-10} \text{ cm}^3 \text{ molecules}^{-1} \text{ s}^{-1}$ ) and  $k_{\text{O}_3}$  ( $2.9 \times 10^{-11} \text{ cm}^3 \text{ molecules}^{-1} \text{ s}^{-1}$ ) bimolecular rate coefficients to form OD are assumed to be equivalent to their hydrogen analogues obtained from the JPL Chemical Kinetics and Photochemical Data evaluation.

The rate equation for the  $\text{CO}_2$  time dependence is

$$\frac{d[\text{CO}_2]}{dt} = k_{1b} [\text{CO}] [\text{OD}]_t - k_{\text{pump}} [\text{CO}_2]_t \quad (\text{S8})$$

The only loss channel for  $\text{CO}_2$  is the gas pump out time ( $k_{\text{pump}}$ ) of the cavity, which is approximately 20 ms.

*OD+CO Chemical Mechanism*



Notes:

- 1) OD are formed in steady-state, especially at longer times. Since we can directly observe OD, we do not need to account for its loss/removal in this scheme.
- 2) We measure the kinetics of DOCOCOCO formation at early times, to minimize biases introduced by secondary reactions, especially radical-radical reactions involving DOCOCOCO.

*Effect of O<sub>3</sub>*: In order to determine the DOCO+O<sub>3</sub> reaction rate, we perform a global fit of  $k_{1a,sum}$  and  $r_{loss,sum}$  across all of the CO, N<sub>2</sub>, D<sub>2</sub>, and O<sub>3</sub> data sets. From this procedure, we obtain an average O<sub>3</sub> loss rate coefficient  $k_{loss,sum} = (2.5 \pm 0.6) \times 10^{-11} \text{ cm}^3 \text{ molecules}^{-1} \text{ s}^{-1}$  (fig. S1). The total loss rate,  $r_{loss,sum}$ , was fixed to this value for the final determination of  $k_{1a,sum}$ . Losses may be isomer specific but are not resolvable with measurement of the total loss. In addition, thermalized *cis*-DOCO loss to D+CO<sub>2</sub> (via tunneling) is expected to be much slower than reaction with O<sub>3</sub>.

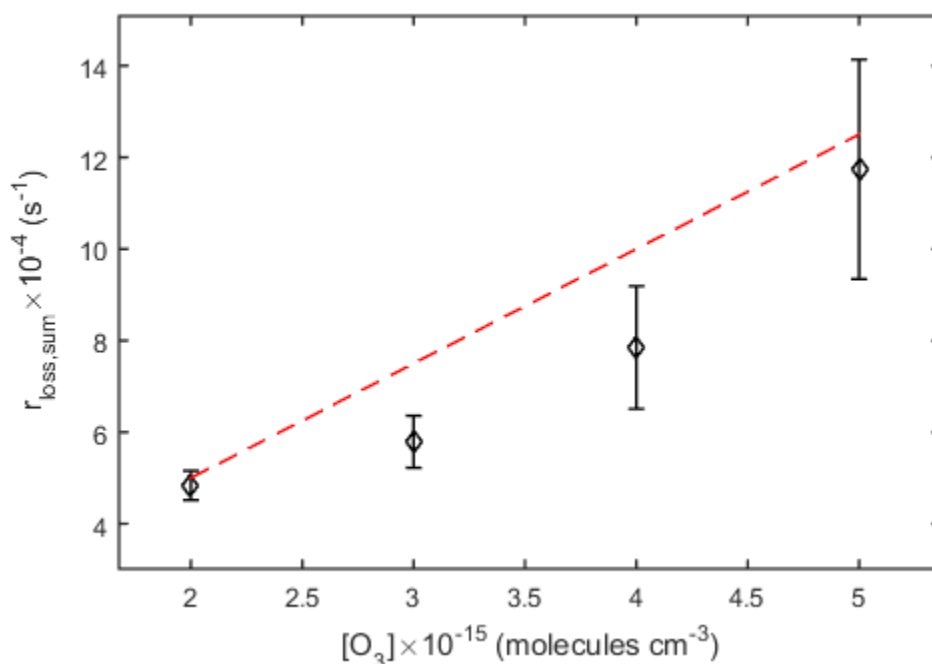


**fig. S1. Variation of  $r_{loss,sum}$  with O<sub>3</sub> concentration.**

*Effect of D<sub>2</sub>*: To determine the impact of D<sub>2</sub> gas on  $k_{1a,sum}$ , we vary D<sub>2</sub> under constant [N<sub>2</sub>]= $9.8 \times 10^{17}$ , [CO]= $5.6 \times 10^{17}$ , and [O<sub>3</sub>]= $2 \times 10^{15}$  molecules cm<sup>-3</sup>. The results are shown in fig. S2. No statistically significant variation with D<sub>2</sub> is observed. Nonetheless, the variation of  $k_{1a,sum}$  with D<sub>2</sub> was included in the multidimensional linear regression, with a fitted rate coefficient of  $k_{1a,sum}^{(D_2)} = 9.6_{-24}^{23} \times 10^{-33} \text{ (cm}^6 \text{ molecules}^{-2} \text{ s}^{-1}\text{)}$ .

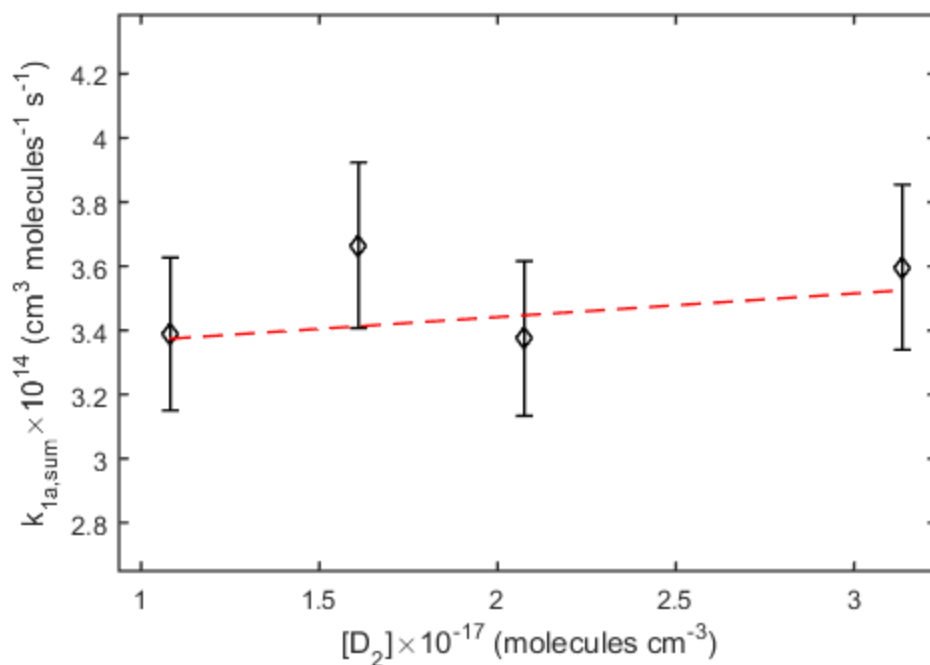


fig. S2. Variation of  $k_{1a,sum}$  with  $D_2$  concentration.

table S4. Summary of statistical and systematic errors for  $k_{1a,sum}$ .

		Error Source	$k_{1a,sum}^{(N_2)}$	$k_{1a,sum}^{(CO)}$
$k_{1a,sum}$ (cm <sup>6</sup> molecules <sup>-2</sup> s <sup>-1</sup> )			$1.3 \times 10^{-32}$	$8.5 \times 10^{-33}$
<b>Statistical Errors</b>		(statistical, fit residual)	15%	47%
<b>Experimental Control</b>	§1	Flow & Pressure	7% (stat)	
<b>Molecular Parameters</b>	§2	OD Cross Section	10% (stat)	
	§2	<i>trans</i> -DOCO Cross Section	10% (stat)	
	§2	<i>cis</i> -DOCO Cross Section	20% (stat)	
<b>Data Analysis</b>		Cross-contamination of OD and D <sub>2</sub> O	-1% (sys)	



		Total Systematic Error	(-11%,+0%)	
		Total Statistical Error	30%, 53%	
		Total Error Budget	(-41%,+30%)	(-64%,+53%)

**table S5. Summary of fitted rate coefficients.**

$k_{1a,sum}^{(CO)}$ (cm <sup>6</sup> molecules <sup>-2</sup> s <sup>-1</sup> )	$8.5_{-5.4}^{4.5} \times 10^{-33}$
$k_{1a,sum}^{(N_2)}$ (cm <sup>6</sup> molecules <sup>-2</sup> s <sup>-1</sup> )	$1.3_{-0.5}^{0.4} \times 10^{-32}$
$k_{1a,sum}^{(D_2)}$ (cm <sup>6</sup> molecules <sup>-2</sup> s <sup>-1</sup> )	$9.6_{-24}^{23} \times 10^{-33}$
$k_{1b}^g$ (cm <sup>3</sup> molecules <sup>-1</sup> s <sup>-1</sup> )	$5.6(7) \times 10^{-14}$
$k_{loss,sum}$ (cm <sup>3</sup> molecules <sup>-1</sup> s <sup>-1</sup> )	$2.5(6) \times 10^{-11}$
$k_{1a,trans}^{(CO)}$ (cm <sup>6</sup> molecules <sup>-2</sup> s <sup>-1</sup> )	$1.4(4) \times 10^{-32}$
$k_{1a,cis}^{(CO)}$ (cm <sup>6</sup> molecules <sup>-2</sup> s <sup>-1</sup> )	$6(2) \times 10^{-33}$
$k_{iso,tc}^{(CO)}$ (cm <sup>3</sup> molecules <sup>-1</sup> s <sup>-1</sup> )	$1.3(2) \times 10^{-13}$
$k_{iso,ct}^{(CO)}$ (cm <sup>3</sup> molecules <sup>-1</sup> s <sup>-1</sup> )	$7.5(2) \times 10^{-13}$

<sup>g</sup>Bui *et al.* 2017

### section S3. Theoretical calculations for OD + CO

*Theoretical rate coefficients for DOCO isomerization:* Using a theoretical technique that combines semi-classical transition state theory (SCTST) with the 2-dimensional master-equations (2DME), we calculate the pressure-dependent *cis*→*trans* and *trans*→*cis* isomerization rate coefficients, denoted as  $k_{iso,ct}$  and  $k_{iso,tc}$ , respectively. This method has previously provided accurate predictions of the pressure-dependent  $k_1(T,P)$  for the OH(OD)+CO reaction. The chemical kinetics analysis is performed using the potential energy surface (PES, Fig. 1) calculated using the HEAT protocol. The third-body collisional partner is air (N<sub>2</sub> = 80%, O<sub>2</sub>=20%). The results are shown in fig. S3. The theoretical equilibrium constant for DOCO isomerization is defined as  $K_{iso,th} = k_{iso,ct}/k_{iso,tc} \approx 14:1$ .

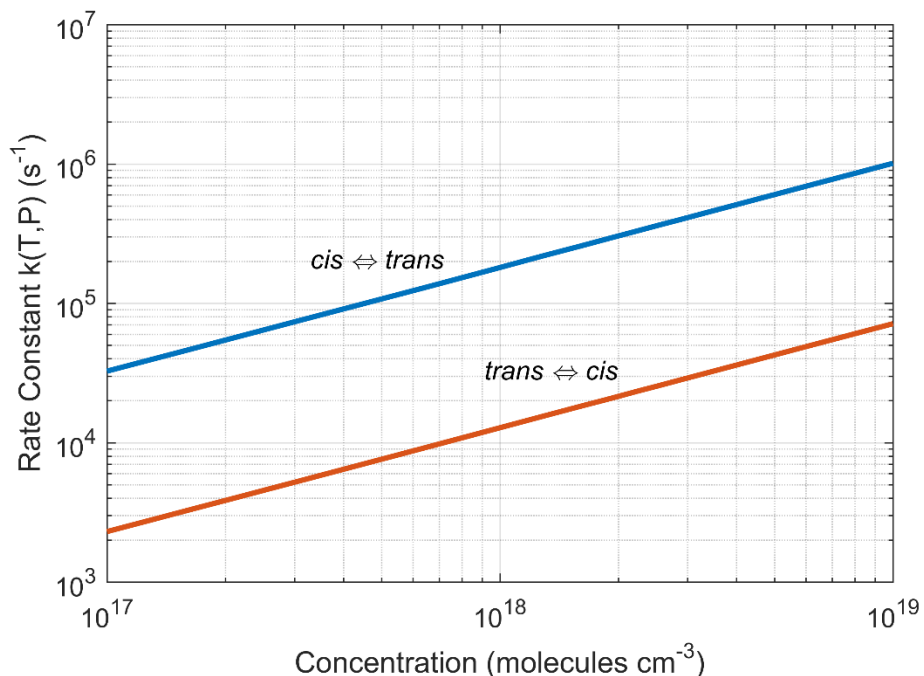


**fig. S3. Calculated *cis/trans* isomerization rates for DOCO isomers using SCTST and 2D master equations.** The calculated  $k(T, P)$  for isomerization (forward and backward) have slopes of less than unity and thus exhibit characteristic “falloff” behavior.

#### section S4. $k_1$ for OD + CO as a function of N<sub>2</sub>

In the low-pressure regime,  $k_1 = k_{1a,cis} + k_{1a,trans} + k_{1b}$ , where  $k_{1b}$  is the bimolecular rate coefficient for the D+CO<sub>2</sub> channel. Using  $k_{1a,cis}$  and  $k_{1a,trans}$  measured in this work,  $k_1$  as a function of N<sub>2</sub> pressure is plotted in green (1 $\sigma$  uncertainty) in fig. S4. The results are in good agreement with  $k_1$  measurements for OD+CO from Golden *et al.* and Paraskevopoulos & Irwin.

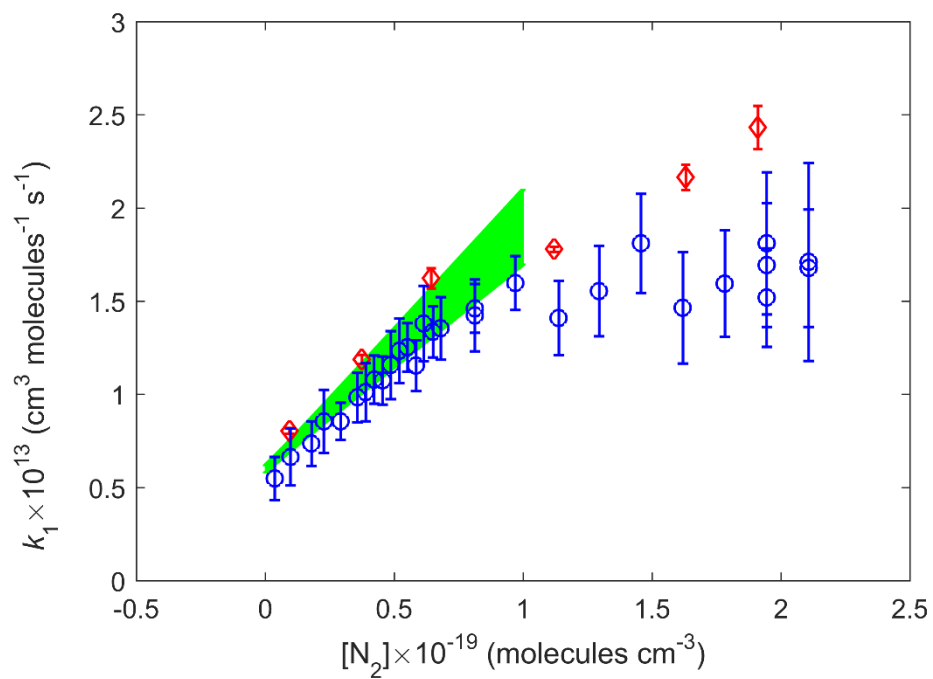


**fig. S4. Measured  $k_1$  comparison with previous works.** The measured  $k_1$  as a function of  $\text{N}_2$  are given by the shaded green region (within  $1\sigma$  uncertainties). Red diamond and blue circles are the measured  $k_1$  values from Golden *et al.* and Paraskevopoulos & Irwin, respectively.